Orientational phase transition between hexagonal solids in planar systems of hard cyclic pentamers and heptamers

2002 J. Phys.: Condens. Matter 14 1261

(http://iopscience.iop.org/0953-8984/14/6/313)

INSTITUTE OF PHYSICS PUBLISHING JOURNAL OF PHYSICS: CONDENSED MATTER

J. Phys.: Condens. Matter **14** (2002) 1261–1273 PII: S0953-8984(02)29297-8

Orientational phase transition between hexagonal solids in planar systems of hard cyclic pentamers and heptamers

K V Tretiakov and K W Wojciechowski[1]

Institute of Molecular Physics, Polish Academy of Sciences, Smoluchowskiego 17/19, 60-179 Poznań, Poland

E-mail: kww@man.poznan.pl

Received 1 October 2001, in final form 10 January 2002
Published 1 February 2002
Online at stacks.iop.org/JPhysCM/14/1261

Abstract

Two-dimensional, hard-body systems of cyclic multimers (pentamers and heptamers) are studied by Monte Carlo simulations. Elastic properties (the elastic constants and the Poisson ratio) are computed for hexagonal solid phases with molecular rotation by using an algorithm based on the strain-fluctuation method. In both systems a minimum of the Poisson ratio is observed at the same density at which a qualitative change of the orientational singlet distribution function occurs. This result confirms that, in each of the studied systems, a phase transition occurs between two elastically isotropic solid phases exhibiting orientational disorder: a higher-density phase with (strongly) hindered rotation and a lower-density phase with (almost) free rotation. The study also suggests that it is worth paying more attention to the dependence of the Poisson ratio on the thermodynamic variables (volume, pressure or temperature) in solids because this quantity can play the role of a sensitive indicator of (at least some) structural phase transitions.

1. Introduction

It is well known that hard-molecule potential, infinite when molecules overlap and zero otherwise, can model various thermodynamically stable and metastable phases both in two and three dimensions. The simplest hard molecules, hard spheres and hard discs, have been used to model simple liquids [1–5], melting process [6,7] and glasses [8]. Hard molecules composed of a few spheres have been applied to study the properties of molecular liquids [9–12]. Other hard molecules convenient to model fluids are hard convex bodies [13] and their generalization, hard star-shaped bodies [14]. Oblate and prolate hard molecules [15–18] as well as hard bodies of more complicated shapes [19–24] have been exploited in computer simulations and theoretical

[1] Author to whom any correspondence should be addressed.

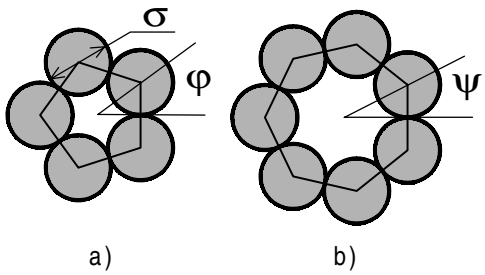

Figure 1. The molecules studied: (a) the hard cyclic *pentamer*, (b) the hard cyclic *heptamer*. The diameter of the discs is σ. (In the text σ is considered as a unit of length.)

studies of liquid crystalline phases. Globular hard molecules have been used to model structural (orientational) phase transitions in solids [16, 25, 26].

Studies of hard-body models have shown that interesting effects can be observed even in two dimensions for as simple molecular shapes as hard cyclic multimers which are composed of identical hard discs ('atoms') centred at vertices of perfect polygons with sides equal to the disc diameter σ. Extensive studies performed for this class of homo-molecular, two-dimensional hard-body systems [25–40] revealed rich phase diagrams [25, 26], unexpected atomic density distributions [27, 35, 36, 40] and have shown that purely geometrical interactions can lead to surprising effects like, for example, phase transitions between solid phases of the same (hexagonal) symmetry [25,28,29], negative Poisson ratio [31,32,38,39] or thermodynamically stable aperiodic solid structures [30, 33, 34, 37]. These results indicate that further studies of the hard cyclic multimer systems are of interest.

In this paper, we consider two planar, hard cyclic multimer systems: hard cyclic pentamers and hard cyclic heptamers, further referred to as pentamers and heptamers, respectively, see figure 1. The pentamer and the heptamer are non-convex but star-shaped molecules [14]. It is worth adding that both these molecules contain axes forbidden in crystals.

It has been suggested that for each of the molecules a phase transition occurs between two (isotropic from the point of view of the elastic properties) rotational phases of different orientational order [36, 38]. It is interesting to know whether such a transition (which is so smooth that it is not seen in the equation of state of the system) influences the elastic properties of the system.

The phase diagram of the pentamer system has already been studied by mechanical simulations [27] and by computer simulations [35, 36, 40]. The mechanical simulations revealed four qualitatively different structures in this system: a high-density anisotropic solid with frozen molecular rotation, two—high-density and low-density—hexagonal solids with rotating molecules, and a fluid at low densities. In the high-density hexagonal solid the 'atomic' density distributions around the lattice sites showed clearly sixfold symmetry and the molecular rotation was strongly hindered. In the low-density hexagonal solid the atomic density profiles around the lattice sites were practically circular and the molecules were rotating almost freely. Only two first-order phase transitions were detected when the structure and equation of state of the system was studied by computer simulations [35]: the first transition corresponded to rotational 'melting' of the anisotropic solid into a hexagonal solid and the second transition corresponded to 'translational' melting of the hexagonal solid into fluid. A careful analysis of the translational–rotational coupling showed, however, a change of the orientational ordering in the system [36] in the density range where a phase transition between strongly hindered and almost free rotation was observed in mechanical simulations.

The system of heptamers has been studied by computer simulations only recently [38]. Its phase diagram is similar to that of the pentamers, except in the highest density range where a few crystalline structures without molecular rotation have been observed, instead of a single one observed in the case of the pentamer system. (The thermodynamic stability ranges of these phases have not yet been fixed.) At the densities below the orientational melting, an analysis of the atomic density distribution around lattice sites in the heptamer system also suggested a continuous phase transition from strongly hindered to almost free rotation in hexagonal solids. Further decrease of the density led to 'translational' melting.

The aim of the present work is twofold. Firstly, by showing that changes of the orientational order in both systems coincide with extrema of their Poisson ratios we provide a new argument in support of a phase transition between hindered and free rotation. (This observation suggests also that the Poisson ratio can play a role of a sensitive indicator of, at least some, structural phase transformations in solids.) Secondly, we present accurate data concerning the values of elastic constants in well defined model systems interacting by anisotropic and extremely anharmonic potentials. These data, which supply information on the convergence of the strain fluctuation method, can be used to test theoretical approximations for calculating the elastic constants of molecular crystals.

2. Simulation technique

The Monte Carlo (MC) method [41] is a particularly simple and efficient technique for studying the equilibrium properties of complex hard-molecule systems when performed at constant pressure. The advantage of this approach with respect to the molecular dynamics is that one avoids integration of complicated equations of motion. One also avoids cumbersome statistical–mechanical calculations which are necessary to compute pressure in the constant-density MC simulations.

Constant-pressure studies of hard-body fluids are usually performed at fixed shape of the periodic box [42]. In solids, however, using variable shape of the periodic box [29] is preferable because the system can then easily eliminate internal strains caused by any misfit of the unit cell and the sample shape. The MC simulations of pentamers and heptamers described in this paper were performed in the NPT ensemble of variable shape. This technique also allows one to easily determine the elastic properties of hard-body systems.

Various methods for simulations of elastic properties of model systems have been proposed [31,43–60]. In general, the methods with fixed shape of the system seem to converge better than those with variable box shape [52]. The former, however, require performance of many runs around the reference state, which must be known (or determined) in advance. Moreover, most of these methods (the exception is the Frenkel–Ladd method [50,60] based on numerical differentiation of the free energy which is computed for a considered system exposed to various deformations around its reference state) require computation of the pressure or even its derivatives [43, 56] which are expressed by rather complicated formulae in the case of anisotropic and non-central molecular interactions.

The present computations of the elastic properties were performed by a version [55] of the strain-fluctuation method [44, 46, 47]. As mentioned above, this method converges more slowly than methods with fixed box shape [45, 59]. This disadvantage is, in our opinion, fully compensated by the simplicity of the method as well as the fact that all the elastic constants are calculated within a single run during which the (equilibrium) reference state is also determined.

To check how the simulation results depend on the number of particles in the system and on the shape of the periodic box, the simulations were carried out for two system shapes, each represented by three system sizes. For the hexagonal phases studied, the

local structure of all the systems studied corresponded to a hexagonal lattice. Samples of the hexagonal lattice of shapes close to the square were chosen to minimize the anisotropy induced by the periodic box. (It is worth mentioning here that large anisotropy of the box may qualitatively modify the thermodynamic properties of the studied system [61,62].) Thus, the average aspect ratio for the systems consisted of $N = 30, 120, 480$ particles was close to $\alpha \equiv L_y/L_x = (6 \times \sqrt{3}/2)/5 = 1.039\,23\ldots$, whereas for the other systems studied, consisting of $N = 56, 224, 896$, it was close to $\alpha = (8 \times \sqrt{3}/2)/7 = 0.989\,74\ldots$. The obtained data were used to estimate values of the computed quantities in the thermodynamic limit. The number of the simulation steps for the studied systems varied from 3×10^6 up to 5×10^7 trial steps per particle (cycles), depending on the system size. Equilibration runs took typically 10% of the simulation length.

3. Orientational probability density

The orientational singlet distribution function (OSDF), normalized to 2π and proportional to the probability density that a particle has a given orientation, provides a basic information on the orientational order. The OSDFs for the systems studied were calculated as histograms from $-C$ to C with a bin length $\Delta = C/83$ (where $C = \pi/5, \pi/7$ for pentamers and heptamers, respectively) and averaged over all the molecules in the system and over the full length of the runs after equilibration.

The OSDF of the pentamer system in the hexagonal crystalline phases with molecular rotation can be well approximated by the function [36]

$$P(\varphi) = 1 + A_{30}\cos(30\varphi) \tag{1}$$

where A_{30} is a coefficient and φ is the orientation of the pentamer molecule. (The coefficient index 30 in (1) comes from the group theoretical analysis: it corresponds to the lowest symmetry axis which contains both the fivefold symmetry axis of the pentamer and the sixfold symmetry axis of the hexagonal lattice.) The fivefold symmetry of the pentamer molecule implies that one can restrict the range of the angle in the OSDF to $\varphi \in (-\pi/5, \pi/5)$.

Similarly, the expression approximating the OSDF of heptamer systems in the hexagonal crystalline phases reads

$$P(\psi) = 1 + A_{42}\cos(42\psi) \tag{2}$$

where A_{42} is a coefficient (the index 42 corresponds to the lowest symmetry axis which contains both the sevenfold symmetry axis of the heptamer and the sixfold symmetry axis of the hexagonal lattice) and ψ is the orientation of the heptamer molecule. The sevenfold symmetry of the heptamer molecule implies that one can restrict the range of the angle to $\psi \in (-\pi/7, \pi/7)$.

Examples of the OSDF for pressures (we use the dimensionless pressure, $p^* = p\sigma^2/k_BT$) representing high-density and low-density hexagonal solids for pentamers and heptamers are shown in figure 2. The values of the coefficients A_{30} and A_{42} decrease with decreasing pressure (or density). For densities $\rho^* \leqslant 0.831(3)$ the pentamer OSDF becomes flat and A_{30} is zero within the accuracy of the experiment, see figure 3(a). Similar behaviour is found in the heptamer systems for the coefficient A_{42} at densities $\rho^* \leqslant 0.880(3)$, see figure 3(b). These results show that at low densities the molecular orientations both in the pentamer system and in the heptamer system are uniformly distributed over the circle. One can see also that the system size does not show noticeable influence on the calculation results of the OSDF and the coefficients A_{30} and A_{42} (see figure 3). So, the present results can be thought of as representative for the thermodynamic limit.

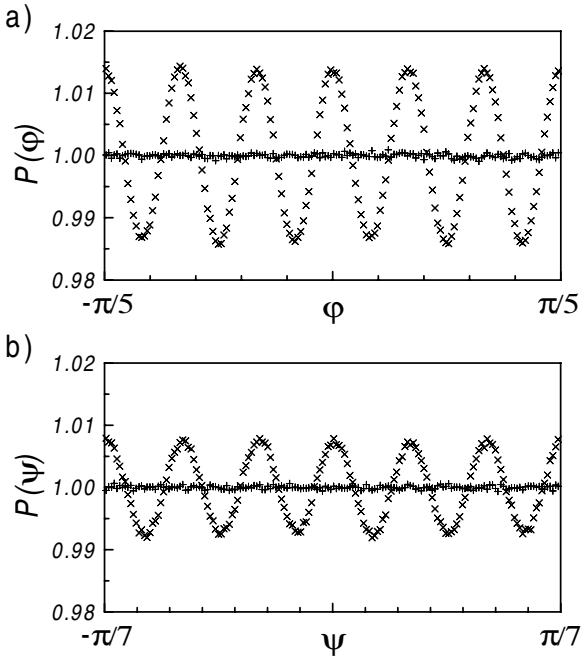

Figure 2. The OSDF: (a) for the pentamers at $p^* = 5$ (×) and at $p^* = 1.8$ (+), (b) for the heptamers at $p^* = 5$ (×) and at $p^* = 1.2$ (+).

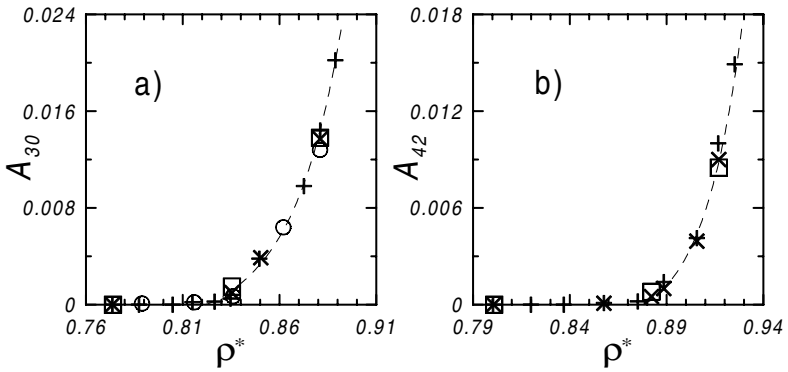

Figure 3. Density dependences of the OSDF constants: (a) A_{30} for pentamers, (b) A_{42} for heptamers. The numbers of particles in the systems are $N = 56$ (+), $N = 224$ (×), $N = 896$ (□). The results obtained in [36] are marked by open circles. The dimensionless density is defined as $\rho^* = \rho/\rho_0$, where ρ_0 is the density at close packing which is $\rho_0^{(5)} \equiv (0.196\,32\ldots)\sigma^{-2}$ [40] for the pentamers and $\rho_0^{(7)} \equiv (0.119\,78\ldots)\sigma^{-2}$ for the heptamers [38, 39].

4. Elastic properties

The studied structures of the orientationally disordered solid phases both for pentamers and heptamers show hexagonal lattices. Such lattices are isotropic from the point of view of the (second order) theory of elasticity [63]. Thus, as in the case of isotropic bodies, their elastic properties can be described by only two elastic moduli [63]. The role of these parameters can

be played, for example, by λ_1 and λ_2 (for other choices of the parameters see below) which are defined by the following free energy expansion

$$\Delta F_{elastic}/V_{ref} = -p(\varepsilon_{xx}+\varepsilon_{yy}) + 2\lambda_1(\varepsilon_{xx}+\varepsilon_{yy})^2 + \lambda_2[(\varepsilon_{xx}-\varepsilon_{yy})^2 + 4\varepsilon_{xy}^2] \tag{3}$$

where $\Delta F_{elastic}$ is the free energy change corresponding to the elastic deformation described by the (Lagrange) strain tensor $\varepsilon_{ij} \equiv (\partial_i x_j + \partial_j x_i + \sum_k \partial_i x_k \partial_j x_k)/2$, and V_{ref} is the volume of the reference state.

At constant pressure it is, however, more convenient to use elastic moduli, $\bar{\lambda}_1$ and $\bar{\lambda}_2$, obtained by the free enthalpy (Gibbs free energy) expansion instead of the free energy expansion [64]. This is so because expanding the free enthalpy at a non-zero pressure one obtains a pure quadratic form (without linear terms) in the strain components:

$$\Delta G/V_p \equiv \Delta(F_{elastic}+pV)/V_p = 2\bar{\lambda}_1(\varepsilon_{xx}+\varepsilon_{yy})^2 + \bar{\lambda}_2[(\varepsilon_{xx}-\varepsilon_{yy})^2 + 4\varepsilon_{xy}^2] \tag{4}$$

where V_p is the volume at equilibrium at the pressure p (reference volume), and V is the volume of the deformed system. There is a simple relation between the bared and not bared elastic moduli [64]:

$$\bar{\lambda}_1 = \lambda_1 \tag{5}$$

$$\bar{\lambda}_2 = \lambda_2 - p/2. \tag{6}$$

The following relations come from equation (4):

$$\langle(\varepsilon_{xx}+\varepsilon_{yy})^2\rangle \equiv \frac{\int d\varepsilon_{xx}\int d\varepsilon_{yy}\int d\varepsilon_{xy}\ (\varepsilon_{xx}+\varepsilon_{yy})^2 \exp(-\Delta G/kT)}{\int d\varepsilon_{xx}\int d\varepsilon_{yy}\int d\varepsilon_{xy}\exp(-\Delta G/kT)} = \frac{kT}{4\bar{\lambda}_1 V_p} \tag{7}$$

$$\langle(\varepsilon_{xx}-\varepsilon_{yy})^2\rangle \equiv \frac{\int d\varepsilon_{xx}\int d\varepsilon_{yy}\int d\varepsilon_{xy}\ (\varepsilon_{xx}-\varepsilon_{yy})^2 \exp(-\Delta G/kT)}{\int d\varepsilon_{xx}\int d\varepsilon_{yy}\int d\varepsilon_{xy}\exp(-\Delta G/kT)} = \frac{T}{2\bar{\lambda}_2 V_p} \tag{8}$$

$$\langle(\varepsilon_{xy})^2\rangle \equiv \frac{\int d\varepsilon_{xx}\int d\varepsilon_{yy}\int d\varepsilon_{xy}\ (\varepsilon_{xy})^2 \exp(-\Delta G/kT)}{\int d\varepsilon_{xx}\int d\varepsilon_{yy}\int d\varepsilon_{xy}\exp(-\Delta G/kT)} = \frac{kT}{8\bar{\lambda}_2 V_p} \tag{9}$$

where k is the Boltzmann constant and T is the temperature.

Introducing the elastic compliances

$$S_{ijkl} = \frac{V_p}{k_B T}\langle\varepsilon_{ij}\varepsilon_{kl}\rangle \tag{10}$$

one obtains

$$\bar{\lambda}_1 = \frac{1}{8(S_{iiii}+S_{xxyy})} \qquad \bar{\lambda}_2 = \frac{1}{4(S_{iiii}-S_{xxyy})} \qquad \bar{\lambda}_2 = \frac{1}{8S_{xyxy}} \tag{11}$$

where $i = x, y$ and the symmetry of the system, leading to $S_{xxxx} = S_{yyyy}$, is exploited; no summation over the repeated indices is performed.

Computation of the averages in the form given by (7)–(9) requires knowing the reference state before the simulations. One can avoid this, however, in the way sketched below.

The integrals over ε_{ij} can be converted to integrals over independent components of the box matrix h_{ij} whose columns are formed by the components of the vectors describing the periodic box [65]. (We should mention here that, as in [55], in this work the box matrix was kept symmetric during the simulations to avoid rotation of the system [66].) The strain tensor can be expressed by the box matrix as follows:

$$\boldsymbol{\varepsilon} \equiv \boldsymbol{\varepsilon}(\boldsymbol{h}) = (\boldsymbol{h}_{ref}^{-1}\cdot\boldsymbol{h}\cdot\boldsymbol{h}\cdot\boldsymbol{h}_{ref}^{-1} - \boldsymbol{I})/2 \tag{12}$$

where $\boldsymbol{h}_{ref}^{-1}$ is the matrix inverse to the reference box matrix $\boldsymbol{h}_{ref}$ which is taken as the average (equilibrium) box matrix, $\boldsymbol{h}_p$, at the pressure p; $\boldsymbol{I}$ is the unit matrix. The average (equilibrium) volume at the pressure p is calculated as

$$V_p = |\langle\det(\boldsymbol{h})\rangle|. \tag{13}$$

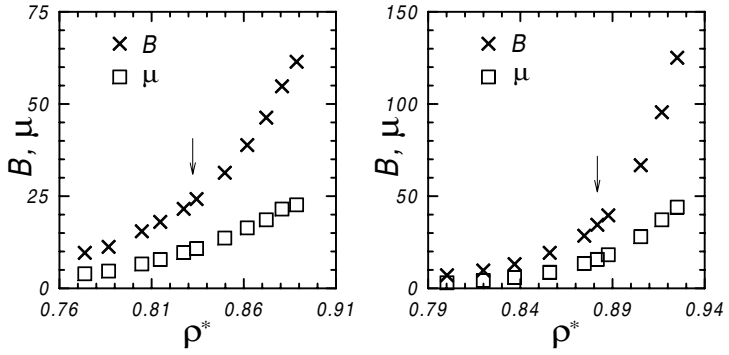

Figure 4. The density dependences of the bulk modulus (×) and the shear modulus (□) of the pentamer systems (left) and the heptamer systems (right) for $N = 56$. Arrows indicate the points where the OSDF functions change character from oscillating to flat.

Denoting the Jacobian of the transformation $\boldsymbol{h} \to \varepsilon$ by $j(\boldsymbol{h})$ one can express the averages in equations (7)–(9) by the ratios of averages with respect to h:

$$\langle \varepsilon_{ij}\varepsilon_{kl}\rangle = \langle \varepsilon_{ij}(\boldsymbol{h})\varepsilon_{kl}(\boldsymbol{h})j(\boldsymbol{h})\rangle_h / \langle j(\boldsymbol{h})\rangle_h. \tag{14}$$

Equation (14) states that the simulation can be performed without knowing the structural parameters of the system at equilibrium. The crucial point here is the fact that 'microscopic enthalpy', $NkT \ln V - U + pV$, can be expressed by the 'instantaneous' components of the box matrix only[2]. ($U \equiv U(\boldsymbol{s}^{(N)}, \boldsymbol{\Omega}^{(N)}, \boldsymbol{h})$ denotes the energy of a configuration of the system, described by the 'normalized' (rescaled) positions of all the particles, $\boldsymbol{s}_i = \boldsymbol{h}^{-1} \cdot \boldsymbol{r}_i (i = 1, \ldots, N)$, their orientations, $\Omega_i (i = 1, \ldots, N)$, and the box matrix $\boldsymbol{h}$.) So, its calculation does not require the knowledge of the reference (equilibrium) state. (This is in contrast to the calculations performed in the constant thermodynamic stress ensemble [53], where the microscopic enthalpy *directly* depends, in general, on the strain tensor components.) Thus, one can perform the simulations without knowing the equilibrium state in advance. The values of the box matrix components, h_{ij}, are stored during the simulations. After finishing the run, the obtained data are analysed and the average (equilibrium) values of the components of the box matrix, $(h_{ref})_{ij}$, are calculated (see the appendix). The calculated equilibrium values are used to compute the strain tensor components, ε_{ij}, which, in turn, makes calculation of the elastic compliances possible.

Remark. We should stress here that the relation (11) holds in the constant-pressure ensemble. For the compliances computed in the constant thermodynamic tension ensemble one should replace the bared moduli by the non-bared ones [53].

The elastic properties of an elastically isotropic system are often described by the bulk modulus, B, and the shear modulus, μ, which are proportional to $\bar{\lambda}_1$ and $\bar{\lambda}_2$, respectively:

$$B = 4\bar{\lambda}_1 \tag{15}$$

$$\mu = 2\bar{\lambda}_2 \equiv 2\lambda_2 - p. \tag{16}$$

Figure 4 shows that B, μ do not exhibit any peculiarities at the densities where one observes the OSDF change from flat to oscillating.

In figure 5 we show λ_1, λ_2 as functions of reduced density. No indications of any phase transition can be seen there.

[2] The microscopic enthalpy is the logarithm of the Boltzmann factor multiplied by kT. In fact, it is enough that the extensive part of the microscopic enthalpy does not depend explicitly on the reference state.

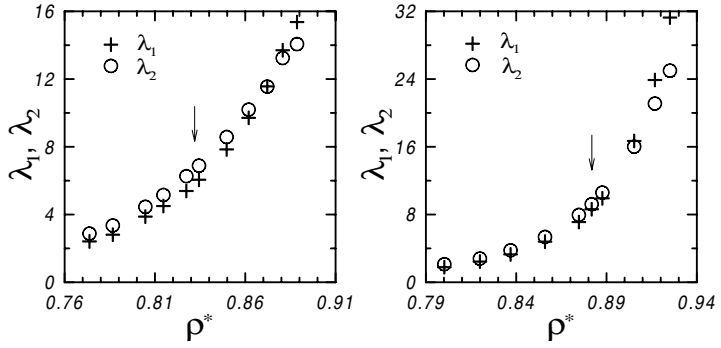

Figure 5. The density dependences of the elastic constants λ_1 (+), λ_2 (○) of the pentamer systems (left) and the heptamer systems (right) for $N = 56$. Arrows indicate the points where the OSDF functions change character from oscillating to flat.

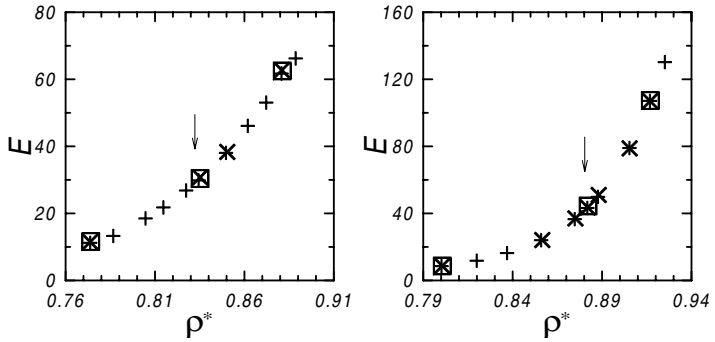

Figure 6. The density dependences of the Young modulus of the pentamer systems (left) and the heptamer systems (right). The numbers of particles in the systems are $N = 56$ (+), $N = 224$ (×), $N = 896$ (□). Arrows indicate the points where the OSDF functions change character from oscillating to flat.

Another way to describe an elastically isotropic system is by using Young's modulus, E, and the Poisson ratio, ν. In figure 6 we show the density dependences of the Young modulus

$$E = \frac{4B\mu}{B+\mu} = \frac{16\bar{\lambda}_1\bar{\lambda}_2}{2\bar{\lambda}_1 + \bar{\lambda}_2} \tag{17}$$

both for pentamers and heptamers. The arrows indicate the densities where the OSDF changes for each system. No indication of any phase transition can be seen there either.

The Poisson ratio is defined as the negative ratio of the transverse strain to the longitudinal strain caused by infinitely small change of the diagonal component of the stress acting in the longitudinal direction [63]. The Poisson ratio of the 2D system under isotropic pressure is [53]

$$\nu = \frac{B-\mu}{B+\mu} = \frac{4\bar{\lambda}_1 - 2\bar{\lambda}_2}{4\bar{\lambda}_1 + 2\bar{\lambda}_2}. \tag{18}$$

The density dependences of the Poisson ratio both for the pentamers and the heptamers are shown in figure 7. It is easy to see there that both these dependences have clear minima. For the pentamer systems the Poisson ratio reaches its minimum at the density $\rho^* \approx 0.830(5)$ (figure 7(a)). As has been mentioned, below this density the particles in the pentamer system show a uniform distribution of orientations over a circle. The Poisson ratio of the heptamer

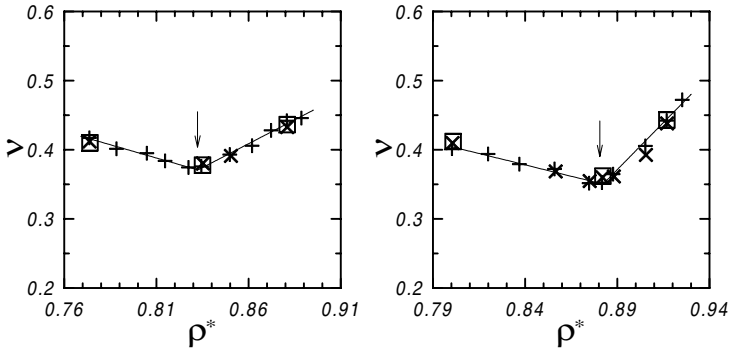

Figure 7. The density dependences of the Poisson ratio of the pentamer systems (left) and the heptamer systems (right). The numbers of particles in the systems are $N = 56$ (+), $N = 224$ ($\times$), $N = 896$ ($\Box$). Arrows indicate the points where the OSDF functions change character from oscillating to flat.

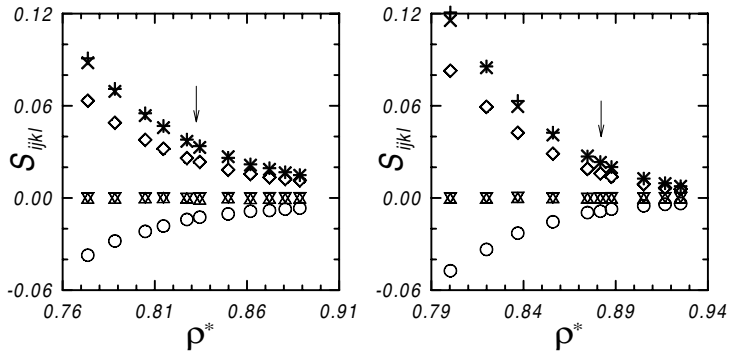

Figure 8. The density dependences of the elastic compliances S_{xxxx} ($\times$), S_{yyyy} (+), S_{xyxy} ($\Diamond$), S_{xxyy} ($\bigcirc$), S_{xxxy} ($\bigtriangledown$), S_{yyxy} ($\bigtriangleup$) of the pentamer systems (left) and the heptamer systems (right). The data presented were obtained for systems which consisted of $N = 56$ particles. Arrows indicate the points where the OSDF functions change character from oscillating to flat.

system reaches its minimum at the density $\rho^* \approx 0.881(5)$, see figure 7(b), which coincides with the density at which the OSDF changes. Thus, in both systems studied, the observed extrema of the Poisson ratio correspond to qualitative changes of the orientational order expressed by the decay of oscillations in the OSDF. This result can be thought of as a new argument confirming the existence of the orientational phase transition in the rotational solids of pentamers and heptamers. As the Poisson ratio, expressed by quantities that are second-order derivatives of the free energy, does not show any discontinuity, this transition should therefore be higher than second order, according to Ehrenfest's classification of phase transitions.

Finally, in figure 8 the density dependences of the elastic compliances S_{ij} are shown. They also do not reveal any peculiarities in the density range studied.

It is worth stressing that the transitions studied are not seen in quantities describing the elastic properties other than the Poisson ratio. This can be understood if one notes that the Poisson ratio is a dimensionless quantity being a *ratio* of the elastic compliances, $\nu = -S_{xxyy}/S_{xxxx}$. Changes of the latter, as well as changes of the elastic constants, in the smooth transitions may be not easily visible, for example, because of their steep dependences on the density or pressure.

Table 1. The elastic moduli of the pentamer systems.

N	p^*	ρ^*	λ_1	λ_2	ν	MC cycles
30	1.8	0.7730(3)	2.43(4)	2.82(5)	0.433(16)	2×10^6
56	1.8	0.7731(3)	2.41(3)	2.88(4)	0.418(12)	3×10^6
120	1.8	0.7733(2)	2.40(5)	2.86(5)	0.420(18)	5×10^6
224	1.8	0.7738(1)	2.44(4)	2.93(4)	0.412(14)	10^7
480	1.8	0.7741(1)	2.43(3)	2.95(3)	0.407(11)	1.5×10^7
896	1.8	0.7741(1)	2.45(2)	2.96(2)	0.408(7)	3×10^7
∞	1.8	0.7742(1)	2.44(3)	2.95(3)	0.408(12)	
30	3.0	0.8338(4)	5.99(8)	6.77(8)	0.389(11)	2×10^6
56	3.0	0.8344(3)	6.05(8)	6.89(10)	0.384(12)	3×10^6
120	3.0	0.8449(3)	6.03(7)	6.98(7)	0.375(10)	5×10^6
224	3.0	0.8350(2)	6.12(7)	7.08(7)	0.374(9)	10^7
480	3.0	0.8351(1)	6.03(7)	7.04(7)	0.370(9)	2×10^7
896	3.0	0.8352(1)	6.10(7)	7.01(7)	0.378(9)	3.5×10^7
∞	3.0	0.8353(1)	6.08(7)	7.06(7)	0.372(9)	
30	5.0	0.8806(4)	13.3(3)	12.9(3)	0.438(20)	2×10^6
56	5.0	0.8808(3)	13.6(3)	13.1(3)	0.439(19)	3×10^6
120	5.0	0.8810(2)	13.5(2)	13.2(2)	0.432(13)	5×10^6
224	5.0	0.8810(2)	13.7(2)	13.4(2)	0.431(13)	10^7
480	5.0	0.8811(1)	13.9(2)	13.2(2)	0.444(13)	2×10^7
896	5.0	0.8811(1)	13.9(2)	13.3(2)	0.440(13)	5×10^7
∞	5.0	0.8812(1)	13.8(2)	13.3(2)	0.438(12)	

Examples of the values obtained for λ_1 and λ_2 in the pentamer systems and in the heptamer system are presented in tables 1 and 2, respectively. It can be seen there that the elastic moduli of both systems depend weakly on the system size. Results obtained for systems as small as $N = 56$ were found to differ by only a few (three) per cent from those obtained by extrapolating a perfect crystal to the thermodynamic limit.

5. Summary and conclusions

MC calculation of the elastic moduli and the Poisson ratio have been carried out in systems of pentamers and heptamers in the density ranges where the molecular rotation is observed in hexagonal solid phases. It has been shown that in both these systems one observes a minimum of the Poisson ratio at the same density where the orientational probability density shows a qualitative change from an oscillating one to a flat one. This fact can be interpreted as a new argument supporting the existence of a phase transition between hindered and free rotation in these systems. Within the Ehrenfest classification, this transition should be of order higher than two.

The present analysis shows that the Poisson ratio is sensitive to rather subtle structural changes (changes of orientational order) in the two-dimensional models studied. The question of to what extent the present result can be generalized on a variety of structural phase transitions which can occur in two and three-dimensional systems remains open. However, the present analysis clearly indicates that the Poisson ratio is worth taking into account in studies of phase transitions in solids. In the context of the observation done by Evans [67] who noticed that '... it is surprising how often the value of ν is not measured but assumed to be about $1/3$ ...' this conclusion may be also of some interest for material scientists.

Table 2. The elastic moduli of the heptamer systems.

N	p^*	ρ^*	λ_1	λ_2	ν	MC cycles
30	1.2	0.7999(5)	1.80(4)	2.00(5)	0.440(21)	2×10^6
56	1.2	0.8000(4)	1.78(3)	2.10(4)	0.407(16)	3×10^6
120	1.2	0.8002(3)	1.80(2)	2.05(6)	0.425(16)	5×10^6
224	1.2	0.8003(2)	1.84(3)	2.14(3)	0.410(14)	10^7
480	1.2	0.8005(1)	1.81(3)	2.14(3)	0.403(14)	1.5×10^7
896	1.2	0.8005(1)	1.85(3)	2.14(3)	0.412(14)	3.5×10^7
∞	1.2	0.8005(1)	1.84(3)	2.14(3)	0.411(13)	
30	2.75	0.8811(3)	8.38(9)	8.94(10)	0.378(9)	2×10^6
56	2.75	0.8817(2)	8.62(8)	9.23(11)	0.374(9)	3×10^6
120	2.75	0.8820(2)	8.75(12)	9.28(12)	0.378(11)	5×10^6
224	2.75	0.8821(1)	8.65(10)	9.36(11)	0.368(10)	10^7
480	2.75	0.8822(1)	8.81(8)	9.51(11)	0.368(8)	2×10^7
896	2.75	0.8823(1)	8.77(8)	9.50(9)	0.367(8)	3.5×10^7
∞	2.75	0.8823(1)	8.78(9)	9.49(10)	0.368(9)	
30	5.0	0.9167(3)	23.8(4)	20.4(4)	0.453(15)	2×10^6
56	5.0	0.9168(2)	23.9(3)	21.1(4)	0.440(13)	3×10^6
120	5.0	0.9169(2)	23.6(3)	21.3(3)	0.430(11)	5×10^6
224	5.0	0.9169(1)	23.7(4)	21.1(4)	0.436(15)	10^7
480	5.0	0.9170(1)	24.1(3)	21.3(3)	0.439(11)	2×10^7
896	5.0	0.9170(1)	24.0(3)	21.1(3)	0.441(11)	3.5×10^7
∞	5.0	0.9170(1)	23.9(3)	21.2(3)	0.438(12)	

Acknowledgments

Part of this work was supported by the Polish Committee for Scientific Research (KBN) within the grant 5 P03B 060 20. Part of the calculations was performed at the Poznań Computer and Networking Centre (PCSS).

Appendix

Some details of computations of the reference box are shown below.

Let $h_{xx}, h_{yy}, h_{xy} = h_{yx}$ denote the 'instantaneous' components of the box matrix. Their average values, H_{xx}, H_{yy}, $H_{xy} = H_{yx}$, define the reference (equilibrium) box matrix:

$$\begin{aligned} H_{ij} \equiv (h_{ref})_{ij} = \langle h_{ij} \rangle &\equiv \frac{\int \mathrm{d}\varepsilon_{xx} \int \mathrm{d}\varepsilon_{yy} \int \mathrm{d}\varepsilon_{xy}\ h_{ij} \exp\left(-\Delta G/kT\right)}{\int \mathrm{d}\varepsilon_{xx} \int \mathrm{d}\varepsilon_{yy} \int \mathrm{d}\varepsilon_{xy} \exp\left(-\Delta G/kT\right)} \\ &= \frac{\int \mathrm{d}h_{xx} \int \mathrm{d}h_{yy} \int \mathrm{d}h_{xy}\ h_{ij}\ j(\boldsymbol{h}) \exp\left(-\Delta G/kT\right)}{\int \mathrm{d}h_{xx} \int \mathrm{d}h_{yy} \int \mathrm{d}h_{xy}\ j(\boldsymbol{h}) \exp\left(-\Delta G/kT\right)} \\ &= \frac{\int \mathrm{d}h_{xx} \int \mathrm{d}h_{yy} \int \mathrm{d}h_{xy}\ h_{ij}\ j(\boldsymbol{h}) \exp\left(-\Delta G/kT\right)}{\int \mathrm{d}h_{xx} \int \mathrm{d}h_{yy} \int \mathrm{d}h_{xy} \exp\left(-\Delta G/kT\right)} \\ &\quad \times \frac{\int \mathrm{d}h_{xx} \int \mathrm{d}h_{yy} \int \mathrm{d}h_{xy} \exp\left(-\Delta G/kT\right)}{\int \mathrm{d}h_{xx} \int \mathrm{d}h_{yy} \int \mathrm{d}h_{xy}\ j(\boldsymbol{h}) \exp\left(-\Delta G/kT\right)} \\ &\equiv \langle h_{ij}\ j(\boldsymbol{h}) \rangle_h \times \frac{1}{\langle j(\boldsymbol{h}) \rangle_h} \end{aligned} \tag{19}$$

where the strain tensor is defined by (12) and, hence, the Jacobian is

$$j(\boldsymbol{h}) \equiv \frac{\partial\left(\varepsilon_{xx}, \varepsilon_{yy}, \varepsilon_{xy}\right)}{\partial\left(h_{xx}, h_{yy}, h_{xy}\right)} = \frac{(h_{xx} + h_{yy})(h_{xy}^2 - h_{xx}h_{yy})}{2(H_{xy}^2 - H_{xx}H_{yy})^3}. \tag{20}$$

Substituting (20) into (19) and cancelling the factors $2(H_{xy}^2 - H_{xx}H_{yy})^3$, which do not depend on the instantaneous configuration of the box, the components of the reference box are given by

$$H_{ij} = \frac{\langle h_{ij}\ (h_{xx} + h_{yy})(h_{xy}^2 - h_{xx}h_{yy})\rangle_h}{\langle (h_{xx} + h_{yy})(h_{xy}^2 - h_{xx}h_{yy})\rangle_h} \tag{21}$$

where

$$\langle f\rangle_h \equiv \frac{\int \mathrm{d}h_{xx} \int \mathrm{d}h_{yy} \int \mathrm{d}h_{xy} V^N \int \mathrm{d}\boldsymbol{s}^{(N)} \int \mathrm{d}\boldsymbol{\Omega}^{(N)}\ f(\boldsymbol{s}^{(N)}, \boldsymbol{\Omega}^{(N)}, \boldsymbol{h})\ \exp(-(U + pV)/kT)}{\int \mathrm{d}h_{xx} \int \mathrm{d}h_{yy} \int \mathrm{d}h_{xy} V^N \int \mathrm{d}\boldsymbol{s}^{(N)} \int \mathrm{d}\boldsymbol{\Omega}^{(N)} \exp(-(U + pV)/kT)}.$$

References

[1] Wood W W and Jacobson J D 1957 *J. Chem. Phys.* **27** 1207
[2] Alder B J and Wainwright T E 1957 *J. Chem. Phys.* **27** 1208
[3] Alder B J and Wainwright T E 1962 *Phys. Rev.* **127** 359
[4] Bernal J D 1964 *Proc. R. Soc.* A **280** 299
[5] Pierański P 1984 *Am. J. Phys.* **52** 68
[6] Alder B J, Hoover W G and Wainwright T E 1963 *Phys. Rev. Lett.* **11** 241
[7] Hoover W G and Ree F H 1968 *J. Chem. Phys.* **49** 3609
[8] Cargill S 1972 *J. Appl. Phys.* **43** 2727
[9] Boublik T 1989 *Mol. Phys.* **68** 191 and references therein
[10] Wertheim M S 1987 *J. Chem. Phys.* **87** 7323 and references therein
[11] Malanoski A P and Monson P A 1997 *J. Chem. Phys.* **107** 6899
[12] Vega C and MacDowell L C 2001 *J. Chem. Phys.* **114** 10 411
[13] Allen M P, Evans G T, Frenkel D and Mulder B 1993 *Adv. Chem. Phys.* **86** 1 and references therein
[14] Wojciechowski K W 1991 *J. Chem. Phys.* **94** 4099
[15] Onsager L 1949 *Ann. NY Acad. Sci.* **51** 3441
[16] Vieillard-Baron J 1972 *J. Chem. Phys.* **56** 4729
[17] Frenkel D and Mulder B M 1985 *Mol. Phys.* **55** 1171
[18] Veerman J A C and Frenkel D 1992 *Phys. Rev.* A **45** 5632
[19] Frenkel D 1991 *Liquids, Freezing and Glass Transition (Les Houches, Session LI)* ed J P Hansen, D Levesque and J Zinn-Justin (Amsterdam: Elsevier)
[20] Evans G T 1992 *Mol. Phys.* **77** 969
[21] Blaak R and Mulder B M 1998 *Phys. Rev.* E **58** 5873
[22] Teixeira P I C, Masters A J and Mulder B M 1998 *Mol. Cryst. Liq. Cryst.* **323** 167
[23] Wojciechowski K W 1998 Liquid crystalline phases of arbitrary point group symmetry with the inversion centre *Statistical Physics: Experiments, Theories and Computer Simulations* ed M Tokuyama and I Oppenheim (Singapore: World Scientific)
[24] Bruinsma R 2001 *Phys. Rev.* E **63** 061705
[25] Brańka A C, Pierański P and Wojciechowski K W 1983 *J. Phys. C: Solid State Phys.* **43** 817
[26] Brańka A C and Wojciechowski K W 1983 *Phys. Rev. Lett.* **50** 846
[27] Brańka A C and Wojciechowski K W 1984 *Phys. Lett.* A **101** 349
[28] Wojciechowski K W and Brańka A C 1984 *J. Phys. C: Solid State Phys.* **43** 817
[29] Wojciechowski K W, Brańka A C and Parrinello M 1984 *Mol. Phys.* **53** 1541
[30] Brańka A C and Wojciechowski K W 1985 *Mol. Phys.* **56** 1419
[31] Wojciechowski K W 1987 *Mol. Phys.* **61** 1247
[32] Wojciechowski K W and Brańka A C 1989 *Phys. Rev.* A **40** 7222
[33] Wojciechowski K W, Frenkel D and Brańka A C 1991 *Phys. Rev. Lett.* **46** 3168
[34] Wojciechowski K W 1991 *Mod. Phys. Lett.* B**5** 1843
[35] Brańka A C and Wojciechowski K W 1991 *Mol. Phys.* **72** 941
[36] Brańka A C and Wojciechowski K W 1993 *Mol. Phys.* **78** 1513
[37] Wojciechowski K W, Brańka A C and Frenkel D 1993 *Physica* A **196**, 519
[38] Wojciechowski K W and Tretiakov K V 2000 *Comput. Methods Sci. Technol.* **6** 101
[39] Tretiakov K V 2000 *PhD Thesis* Institute of Molecular Physics, Polish Academy of Sciences, Poznań
[40] Tretiakov K V and Wojciechowski K W 2001 *TASK Quarterly* **5** 331
[41] Metropolis Q W, Metropolis M N, Rosenbluth A H, Teller A H and Teller E 1953 *J. Chem. Phys.* **21** 1087

[42] McDonald I R 1972 *Mol. Phys.* **23** 41
[43] Squire D R, Holt A C and Hoover W G 1968 *Physica* **42** 388
[44] Parrinello M and Rahman A 1982 *J. Chem. Phys.* **76** 2662
[45] Sprik M, Impey R W and Klein M L 1984 *Phys. Rev.* A **29** 4368
[46] Ray J R and Rahman A 1984 *J. Chem. Phys.* **80** 4423
[47] Ray J R and Rahman A 1985 *J. Chem. Phys.* **82** 4243
[48] Ray J R, Moody M C and Rahman A 1985 *Phys. Rev.* B **32** 733
[49] Ray J R, Moody M C and Rahman A 1986 *Phys. Rev.* B **33** 895
[50] Frenkel D and Ladd A J C 1987 *Phys. Rev. Lett.* **559** 1169
[51] Runge K J and Chester G V 1987 *Phys. Rev.* A **36** 4852
[52] Çagin T and Ray J R 1988 *Phys. Rev.* B **38** 7940
[53] Wojciechowski K W and Brańka A C 1989 *Phys. Lett.* A **134** 314
[54] Boal D H, Seifert U and Schillcock J C 1993 *Phys. Rev.* E **48** 4274
[55] Wojciechowski K W and Tretiakov K V 1999 *Comput. Phys. Commun.* **121–2** 528
[56] Farago O and Kantor Y 2000 *Phys. Rev.* E **61** 2478
[57] Sengupta S, Nielaba P, Rao M and Binder K 2000 *Phys. Rev.* E **61** 1072
[58] Sengupta S, Nielaba P and Binder K 2000 *Phys. Rev.* E **61** 6294
[59] Zhou Z 2001 *J. Chem. Phys.* **114** 8769
[60] Bates M A and Frenkel D 2001 *Phys. Rev.* E **61** 5223
[61] Wojciechowski K W, Pieranski P and Malecki J 1982 *J. Chem. Phys.* **76** 6170
[62] Wojciechowski K W, Pieranski P and Malecki J 1983 *J. Phys. A: Math. Gen.* **16** 2197
[63] Landau L D and Lifshitz E M 1959 *Theory of Elasticity* (Oxford: Pergamon)
[64] Wojciechowski K W 1995 *Mol. Phys. Rep.* **10** 129
[65] Parrinello M and Rahman A 1981 *J. Appl. Phys.* **52** 7182
[66] Nose S and Klein M L 1983 *Mol. Phys.* **50** 1055
[67] Evans K E 1991 *Endeavour, New Series* **15** 170